CHEMISTRY OF MATERIALS
Article

Chem. Mater. **2010,** *22,* 1673–1679 1673
DOI:10.1021/cm903067a

Phenyl vs Alkyl Polythiophene: A Solar Cell Comparison Using a Vinazene Derivative as Acceptor

Claire H. Woo,[†] Thomas W. Holcombe,[†] David A. Unruh,[†] Alan Sellinger,[‡] and Jean M. J. Fréchet*,[†]

[†]*Materials Sciences Division, Lawrence Berkeley National Laboratory, Berkeley, California 94720, and College of Chemistry, University of California, Berkeley, California 94720-1460 and* [‡]*Department of Materials Science and Engineering, Stanford University, Stanford, California 94305*

Received October 2, 2009. Revised Manuscript Received December 11, 2009

The solar cell performance of poly[3-(4-n-octyl)-phenylthiophene] (POPT) and poly(3-hexylthiophene) (P3HT) are compared in devices using 4,7-bis(2-(1-(2-ethylhexyl)-4,5-dicyanoimidazol-2-yl)vinyl)benzo[c][1,2,5]-thiadiazole (EV-BT) as the electron acceptor. Despite their reduced light absorption, POPT:EV-BT devices generate higher photocurrents in both bilayer and bulk heterojunction (BHJ) architectures than analogous P3HT:EV-BT devices. Optimized POPT:EV-BT BHJ devices achieve 1.4% average efficiency, whereas the analogous P3HT devices only reach 1.1%. Morphology does not account for the large difference in performance as AFM studies of the active layer suggest comparable levels of phase separation in the two systems. Reverse bias analysis demonstrates that P3HT devices have a higher maximum potential than POPT devices, but P3HT devices appear to be more severely limited by recombination losses under standard operating conditions. A possible explanation for the superior performance in POPT devices is that the pendant phenyl ring in POPT can twist out-of-plane and increase the separation distance with the acceptor molecule. A larger donor/acceptor separation distance can destabilize the geminate pair and lead to more efficient charge separation in POPT:EV-BT devices. Our results emphasize the importance of donor/acceptor pair interactions and its effect on charge separation processes in polymer solar cells.

Introduction

Conjugated polymers offer great promise for realizing low cost, solution processable organic photovoltaics (OPVs).[1−3] Recent progress of OPV efficiencies over 6% for polymers and 4% for small molecules have been reported.[4−6] In the past few years, research efforts have focused on increasing the active layer absorption to improve power conversion efficiency, either by developing low band gap polymers that have greater spectral breaths[7−10] or by replacing [6,6]-phenyl-C_{61}-butyric acid methyl ester ($PC_{61}BM$) with more light-absorbing acceptors.[11−14] Recent reports have also suggested that recombination (geminate and/or bimolecular) is a major loss mechanism in OPV operation.[15−18] Thus, the study of charge separation dynamics in polymers, especially in devices that utilize nonfullerene based acceptors, is increasingly important for understanding and ultimately overcoming current limitations in OPVs.

Poly(3-hexylthiophene) (P3HT) is a semiconducting polymer that has been studied extensively for application in OPVs, achieving ∼4% power conversion efficiency (PCE) in bulk heterojunction (BHJ) devices using the

*Corresponding author e-mail: frechet@berkeley.edu.

(1) Thompson, B. C.; Fréchet, J. M. J. *Angew. Chem., Int. Ed.* **2008**, *47*, 58–77.
(2) Dennler, G.; Scharber, M. C.; Brabec, C. J. *Adv. Mater.* **2009**, *21*, 1323–1338.
(3) Chen, L. M.; Hong, Z. R.; Li, G.; Yang, Y. *Adv. Mater.* **2009**, *21*, 1434–1449.
(4) Hou, J. H.; Chen, H. Y.; Zhang, S. Q.; Chen, R. I.; Yang, Y.; Wu, Y.; Li, G. *J. Am. Chem. Soc.* **2009**, *131*, 15586–15587.
(5) Chen, H. Y.; Hou, J.; Zhang, S.; Liang, Y.; Yang, G.; Yang, Y.; Yu, L.; Wu, Y.; Li, G. *Nat. Photonics* **2009**, *3*, 649–653.
(6) Walker, B.; Tamayo, A. B.; Dang, X. D.; Zalar, P.; Seo, J. H.; Garcia, A.; Tantiwiwat, M.; Nguyen, T. Q. *Adv. Funct. Mater.* **2009**, *19*, 3063–3069.
(7) Liang, Y.; Feng, D.; Wu, Y.; Tsai, S. T.; Li, G.; Ray, C.; Yu, L. *J. Am. Chem. Soc.* **2009**, *131*, 7792–7799.
(8) Wienk, M. M.; Turbiez, M.; Gilot, J.; Janssen, R. A. J. *Adv. Mater.* **2008**, *20*, 2556–2560.
(9) Peet, J.; Kim, J. Y.; Coates, N. E.; Ma, W. L.; Moses, D.; Heeger, A. J.; Bazan, G. C. *Nat. Mater.* **2007**, *6*, 497–500.
(10) Hou, J.; Chen, H. Y.; Zhang, S.; Li, G.; Yang, Y. *J. Am. Chem. Soc.* **2008**, *130*, 16144–16145.
(11) Park, S. H.; Roy, A.; Beaupre, S.; Cho, S.; Coates, N.; Moon, J. S.; Moses, D.; Leclerc, M.; Lee, K.; Heeger, A. J. *Nat. Photonics* **2009**, *3*, 297–303.
(12) Zhan, X. W.; Tan, Z. A.; Domercq, B.; An, Z. S.; Zhang, X.; Barlow, S.; Li, Y. F.; Zhu, D. B.; Kippelen, B.; Marder, S. R. *J. Am. Chem. Soc.* **2007**, *129*, 7246–7247.
(13) Koetse, M. M.; Sweelssen, J.; Hoekerd, K. T.; Schoo, H. F. M.; Veenstra, S. C.; Kroon, J. M.; Yang, X. N.; Loos, J. *Appl. Phys. Lett.* **2006**, *88*, 083504.
(14) Kietzke, T.; Hörhold, H. H.; Neher, D. *Chem. Mater.* **2005**, *17*, 6532–6537.
(15) Lenes, M.; Morana, M.; Brabec, C. J.; Blom, P. W. M. *Adv. Funct. Mater.* **2009**, *19*, 1106–1111.
(16) Hwang, I. W.; Moses, D.; Heeger, A. J. *J. Phys. Chem. C* **2008**, *112*, 4350–4354.
(17) Ohkita, H.; Cook, S.; Astuti, Y.; Duffy, W.; Tierney, S.; Zhang, W.; Heeney, M.; McCulloch, I.; Nelson, J.; Bradley, D. D. C.; Durrant, J. R. *J. Am. Chem. Soc.* **2008**, *130*, 3030–3042.
(18) Clarke, T. M.; Ballantyne, A. M.; Nelson, J.; Bradley, D. D. C.; Durrant, J. R. *Adv. Funct. Mater.* **2008**, *18*, 4029–4035.

Published on Web 01/08/2010

fullerene derivative $PC_{61}BM$ as the acceptor.[19,20] Substituting the solubilizing alkyl chain with a phenyl-alkyl group significantly alters the optoelectronic properties of the polythiophene and its device performance in solar cells.[21−24] For example, compared to P3HT, poly[3-(4-n-octyl)-phenylthiophene] (POPT) exhibits a smaller optical band gap of 1.8 eV, while its lower lying HOMO improves its air stability.[25,26]

A recent report has demonstrated the improved device performance of POPT over P3HT using a cyano-substituted polyphenylene-vinylene as the electron acceptor in an all-polymer bilayer solar cell.[24] The higher extracted photocurrent of POPT devices was not expected from considerations of absorption and energy levels, suggesting that there are other important factors affecting charge separation that have been largely ignored in the field of polymer OPVs. However, the use of acceptor polymers in combination with donor polymers are often limited by thermodynamics as two polymers tend to phase separate affording micrometer-size domains that lead to morphologies unfavorable for BHJ devices. Thus all-polymer BHJ solar cells have only shown limited efficiencies, and most reports have focused on bilayer devices.[12−14,27,28] On the other hand, small molecule acceptors offer the advantage of increased miscibility with various donor polymers, which facilitates the fabrication of BHJ devices.[29] In this study, we chose a small molecule derivative of vinazene as the acceptor in solar cell devices in order to compare the performance of POPT and P3HT. Vinazene derivatives are a new class of acceptor materials that have been shown to achieve efficiencies ranging from 0.45% to 0.94% in devices with various donor polymers.[30−33] With easily tunable absorption, energy levels, and solubility, vinazenes provide a convenient platform to investigate polymer OPV operation with the potential to yield improved performance over fullerenes.[34,35]

Herein, we report the solar cell performance of P3HT and POPT, both synthesized via Grignard metathesis (GRIM) polymerization, using the vinazene derivative 4,7-bis(2-(1-(2-ethylhexyl)-4,5-dicyanoimidazol-2-yl)vinyl)-benzo[c][1,2,5]-thiadiazole (EV-BT) as the electron acceptor. We also provide a performance comparison with devices prepared from Rieke P3HT, which is considered the standard for state-of-the-art P3HT:PCBM solar cells.[19,20]

Experimental Section

The detailed syntheses of GRIM P3HT, POPT, and EV-BT have been reported elsewhere.[24,34−36] Rieke P3HT was purchased from Rieke Metals, Inc. and was used without further purification. Anhydrous solvents were used for the preparation of spin coating solutions.

Cyclic voltammograms were collected using a Solartron 1285 potentiostat under the control of CorrWare II software. A standard three electrode cell based on a Pt wire working electrode, a silver wire pseudo reference electrode (calibrated vs Fc/Fc+), and a Pt wire counter electrode was purged with nitrogen and maintained under a nitrogen atmosphere during all measurements. Dry acetonitrile purged with nitrogen prior to use and tetrabutyl ammonium hexafluorophosphate (0.1 M) was used as the supporting electrolyte. Polymer films were cast onto a Pt wire working electrode from a 1% (w/w) chloroform solution and dried under nitrogen prior to measurement.

UV−visible absorption spectra were obtained using a Cary 50 Conc UV−visible spectrophotometer in transmission geometry. For thin film measurements polymers were spin coated from chlorobenzene solutions onto cleaned glass slides. A model P6700 Spincoater was used to spin coat the films at 2000 rpm for 60 s. Polymer film thickness was measured by a Veeco Dektak profilometer.

Polymer mobility was measured using a diode configuration of ITO/ PEDOT:PSS/ Polymer/Al in the space charge limited current (SCLC) regime. At sufficient potential the conduction of charges in the device can be described by

$$J_{SCLC} = \frac{9}{8}\varepsilon\varepsilon_o\mu\frac{V^2}{L^3} \quad (1)$$

where ε_0 is the permittivity of free space, ε is the dielectric constant of the polymer, μ is the mobility of the majority charge carriers, V is the potential across the device ($V = V_{applied} - V_{bi}$ - V_r), and L is the polymer layer thickness. The series and contact resistance of the device (~15 Ω) was measured using a blank device (ITO/PEDOT/Al), and the voltage drop due to this resistance (V_r) was subtracted from the applied voltage. The built-in voltage (V_{bi}), which is based on the relative work function difference of the two electrodes, was also subtracted from the applied voltage. The built-in voltage can be determined from the transition between the Ohmic region and the SCLC region and was found to be about 1 V.

All photovoltaic devices have a layered structure with the photoactive layer sandwiched between the two electrodes, ITO

(19) Ma, W. L.; Yang, C. Y.; Gong, X.; Lee, K.; Heeger, A. J. *Adv. Funct. Mater.* **2005**, *15*, 1617–1622.
(20) Li, G.; Shrotriya, V.; Huang, J. S.; Yao, Y.; Moriarty, T.; Emery, K.; Yang, Y. *Nat. Mater.* **2005**, *4*, 864–868.
(21) Gadisa, A.; Svensson, M.; Andersson, M. R.; Inganäs, O. *Appl. Phys. Lett.* **2004**, *84*, 1609–1611.
(22) Pei, Q.; Järvinen, H.; Österholm, J. E.; Inganäs, O.; Laakso, J. *Macromolecules* **1992**, *25*, 4297–4301.
(23) Chen, L. C.; Godovsky, D.; Inganäs, O.; Hummelen, J. C.; Janssens, R. A. J.; Svensson, M.; Andersson, M. R. *Adv. Mater.* **2000**, *12*, 1367–1370.
(24) Holcombe, T. W.; Woo, C. H.; Kavulak, D. F. J.; Thompson, B. C.; Fréchet, J. M. J. *J. Am. Chem. Soc.* **2009**, *131*, 14160–14161.
(25) Johansson, T.; Mammo, W.; Svensson, M.; Andersson, M. R.; Inganäs, O. *J. Mater. Chem.* **2003**, *13*, 1316–1323.
(26) Brabec, C. J.; Winder, C.; Scharber, M. C.; Sariciftci, N. S.; Hummelen, J. C.; Svensson, M.; Andersson, M. R. *J. Chem. Phys.* **2001**, *115*, 7235–7244.
(27) McNeill, C. R.; Abrusci, A.; Zaumseil, J.; Wilson, R.; McKiernan, M. J.; Burroughes, J. H.; Halls, J. J. M.; Greenham, N. C.; Friend, R. H. *Appl. Phys. Lett.* **2007**, *90*, 193506.
(28) Alam, M. M.; Jenekhe, S. A. *Chem. Mater.* **2004**, *16*, 4647–4656.
(29) Lim, Y. F.; Shu, Y.; Parkin, S. R.; Anthony, J. E.; Malliaras, G. G. *J. Mater. Chem.* **2009**, *19*, 3049–3056.
(30) Ooi, Z. E.; Tam, T. L.; Shin, R. Y. C.; Chen, Z. K.; Kietzke, T.; Sellinger, A.; Baumgarten, M.; Mullen, K.; deMello, J. C. *J. Mater. Chem.* **2008**, *18*, 4619–4622.
(31) Kietzke, T.; Shin, R. Y. C.; Egbe, D. A. M.; Chen, Z. K.; Sellinger, A. *Macromolecules* **2007**, *40*, 4424–4428.
(32) Schubert, M.; Yin, C.; Castellani, M.; Bange, S.; Tam, T. L.; Sellinger, A.; Hörhold, H. H.; Kietzke, T.; Neher, D. *J. Chem. Phys.* **2009**, *130*, 094703.
(33) Inal, S.; Castellani, M.; Sellinger, A.; Neher, D. *Macromol. Rapid Commun.* **2009**, *30*, 1263–1268.
(34) Shin, R. Y. C.; Kietzke, T.; Sudhakar, S.; Dodabalapur, A.; Chen, Z. K.; Sellinger, A. *Chem. Mater.* **2007**, *19*, 1892–1894.
(35) Shin, R. Y. C.; Sonar, P.; Siew, P. S.; Chen, Z. K.; Sellinger, A. *J. Org. Chem.* **2009**, *74*, 3293–3298.
(36) Watanabe, N.; Mauldin, C.; Fréchet, J. M. J. *Macromolecules* **2007**, *40*, 6793–6795.

Table 1. Characterizations of the Three Polymers Used in This Study

	M_n (g/mol)	PDI	RR	absorption coefficient α at λ_{max} ($\times 10^4$ cm^{-1})	μ_{hole} (cm^2/(V s))	HOMO (eV)	LUMO (eV)
POPT	66,600	1.09	99%	4.1	1×10^{-4}	5.5	3.2
GRIM P3HT	37,700	1.04	99%	8.1	1×10^{-4}	5.2	3.2
Rieke P3HT	28,700	3.48	95%	6.7	1×10^{-4}	5.2	3.2

and LiF/Al. Glass substrates coated with a 150 nm sputtered ITO pattern of 20 Ω □$^{-1}$ resistivity were obtained from Thin Film Device, Inc. The ITO-coated glass substrates were ultrasonicated for 20 min each in acetone and then in 2% Hellmanex soap water, followed by extensive rinsing and ultrasonication in deionized water and then isopropyl alcohol. The substrates were then dried under a stream of dry nitrogen. A dispersion of PEDOT:PSS (Baytron PH500) in water was filtered (0.45 μm glass) and spin coated at 4000 rpm for 60 s, affording a ~30 nm layer. The substrates were dried for 10 min at 140 °C in air and then transferred into an argon glovebox for subsequent procedures. Polymer solutions were prepared in chlorobenzene at a concentration of 10 mg/mL and were heated to 120 °C overnight for complete dissolution. Polymer solutions were added to preweighed EV-BT to yield blend solutions of different concentrations and mixing ratios. For thinner devices, the stock solutions were diluted with chlorobenzene. The active layer was spin coated at 1200 rpm for 60 s on top of the PEDOT:PSS layer. Bilayer devices were fabricated via two spin coating steps using chlorobenzene as the solvent for the bottom polymer layer and THF as the solvent for the EV-BT top layer. THF was chosen as the solvent for EV-BT because GRIM P3HT and POPT were insoluble in THF. The substrates were then placed in an evaporation chamber and pumped down to a pressure of ~5 × 10^{-6} Torr before evaporating a 1 nm LiF layer and subsequently a 100 nm Al layer through a shadow mask on top of the photoactive layer. Two different shadow masks were used to yield devices with active areas of 0.03 cm^2 and 0.16 cm^2. The mechanical removal of part of the organic layer allowed contact with the ITO and adding conductive Ag paste to the removed area to ensure electrical contact completed the device. Testing of the devices was performed under an argon atmosphere with an Oriel Xenon arc lamp having an AM 1.5G solar filter to yield 100 mW cm^{-2} light intensity as calibrated by an NREL certified silicon photocell. Current−voltage behavior was measured with a Keithley 236 SMU. Eight devices were averaged for each condition.

The external quantum efficiency (EQE) was determined at zero bias by illuminating the device with monochromatic light supplied by a Xenon lamp in combination with a monochromator (Spectra Pro 150, Acton Research Corporation). The number of photons incident on the sample was calculated for each wavelength by using a Si photodiode calibrated by the manufacturer (Hamamatsu).

Atomic force microscopy (AFM) was performed to study the surface morphology of the polymer:EV-BT blends. Topographical and phase images were obtained concurrently using a Veeco Multimode V AFM in tapping mode using RTESP tips.

Results

The chemical structures of the materials used in this study are shown in Figure 1, and characterization data for the polymers are included in Table 1. It should be noted that both GRIM P3HT and POPT are highly regioregular (RR) and require heating to completely dissolve in chlorobenzene at higher concentrations. The limited solubility

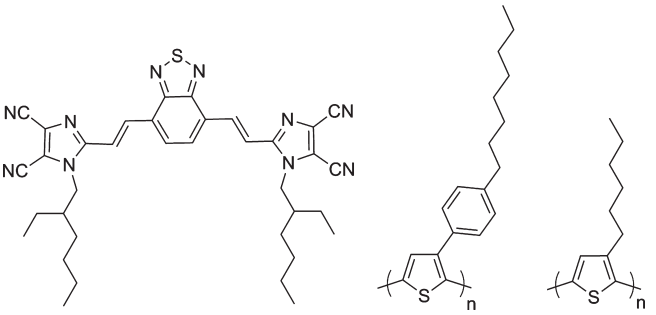

Figure 1. Chemical structures of EV-BT, POPT, and P3HT.

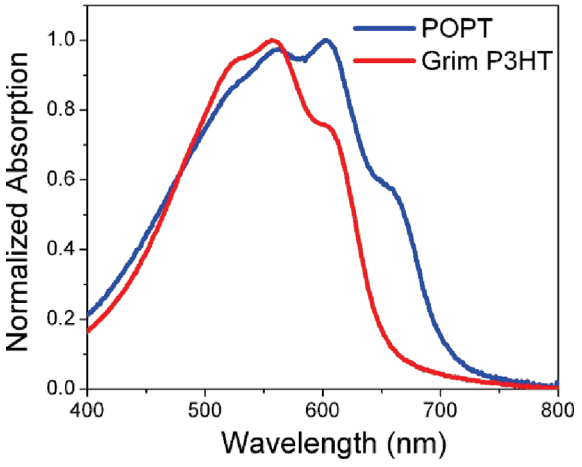

Figure 2. Normalized solid state absorption of POPT and GRIM P3HT.

of GRIM P3HT and POPT in other organic solvents also enables the fabrication of bilayer solar cells using THF as the orthogonal solvent to spin-coat a layer of EV-BT on top of the previously spin-coated polymer layer.

The absorption coefficients α shown in Table 1 are measured by varying the polymer film thickness from 5−60 nm and examining the change in intensity of their absorption maximum λ_{max}. The α values are measured to be 8.1 × 10^4 cm^{-1} for GRIM P3HT and 4.1 × 10^4 cm^{-1} for POPT. The 50% reduction in optical density in POPT is likely due to the phenyl ring twisting out of plane from the thiophene backbone, which leads to increased spacing between the polymer backbones.[37] As shown in the absorption spectra of Figure 2, POPT has greater spectral breath with an absorption onset at 700 nm (1.8 eV) compared to 650 nm (1.9 eV) for P3HT. The space-charge limited hole mobility of the two polymers are similar, both on the order of 1 × 10^{-4} cm^2/(V s). The energy levels of the polymers as measured by cyclic voltammetry (CV) are also shown in Table 1. GRIM P3HT has a HOMO

(37) Fell, H. J.; Samuelsen, E. J.; Andersson, M. R.; Alsnielsen, J.; Grübel, G.; Mårdalen, J. *Synth. Met.* **1995**, *73*, 279–283.

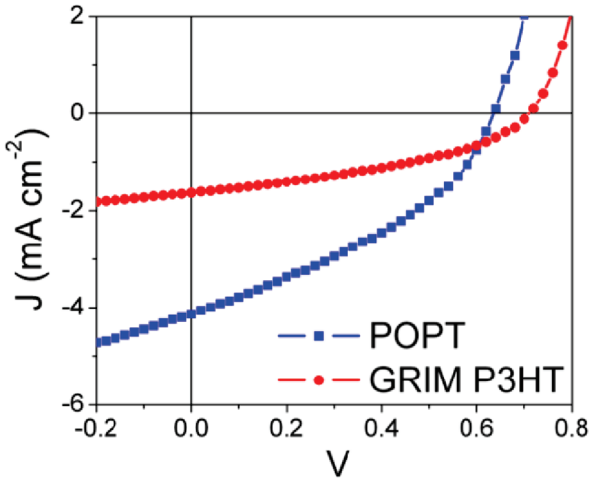

Figure 3. Typical *J-V* characteristics of bilayer devices made from POPT and GRIM P3HT using EV-BT as the top acceptor layer. Devices were annealed at 80 °C for 20 min. Average device parameters: V_{oc} = 0.64, J_{sc} = 4.0 mA cm^{-2}, FF = 0.38, PCE = 0.97% for POPT/EV-BT; V_{oc} = 0.70, J_{sc} = 1.7 mA cm^{-2}, FF = 0.36, PCE = 0.43% for GRIM P3HT/ EV-BT.

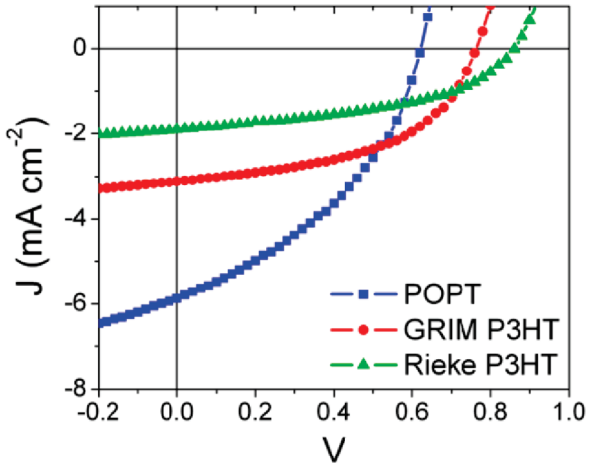

Figure 4. Typical *J-V* characteristics of BHJ solar cells comparing POPT, GRIM P3HT, and Rieke P3HT with a 1:1 weight ratio of polymer to EV-BT and annealed at 80 °C for 40 min. Average device parameters: V_{oc} = 0.62, J_{sc} = 5.5 mA cm^{-2}, FF = 0.40, PCE = 1.4% for POPT:EV-BT; V_{oc} = 0.76, J_{sc} = 3.0 mA cm^{-2}, FF = 0.48, PCE = 1.1% for GRIM P3HT:EV-BT; V_{oc} = 0.84, J_{sc} = 1.9 mA cm^{-2}, FF = 0.44, PCE = 0.70% for Rieke P3HT:EV-BT.

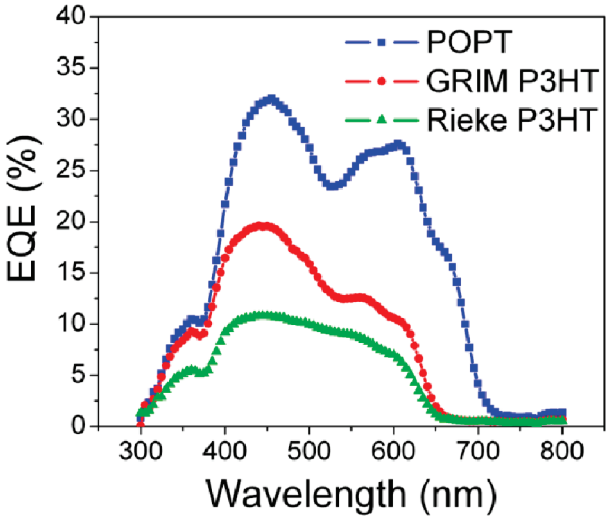

Figure 5. EQE spectra of optimized BHJ devices of POPT, GRIM P3HT, and Rieke P3HT measured at 0 V. All devices have a 1:1 weight ratio of polymer to EV-BT and were annealed at 80 °C for 40 min.

level of 5.2 eV, whereas POPT has a lower HOMO of 5.5 eV. Both polymers have a similar LUMO level of 3.2 eV.

Figure 3 shows typical *J-V* characteristics of bilayer devices fabricated from POPT and GRIM P3HT using EV-BT as the electron acceptor layer spun out of THF. The device structure is ITO/ PEDOT:PSS (30 nm)/POPT or GRIM P3HT (40 nm)/ EV-BT (40 nm)/ LiF (1 nm)/ Al (100 nm). Upon annealing at 80 °C for 20 min, the POPT devices reach an average efficiency of 0.97%, which is more than twice that of GRIM P3HT devices with an average of 0.43%. The higher efficiency of the POPT device originates from an improvement in the photocurrent as the short-circuit current (J_{sc}) is 4.0 mA cm^{-2} compared to only 1.7 mA cm^{-2} for the GRIM P3HT device. It is interesting to note that the POPT device has a slightly lower V_{oc} of 0.64 V compared to 0.70 V for GRIM P3HT device despite POPT having a lower HOMO level of 0.3 eV (−5.5 vs −5.2 eV) as determined from cyclic voltammetry.

BHJ devices have also been fabricated varying annealing conditions, device thickness, and the weight ratio of polymer to EV-BT. The optimal device thickness is 80−100 nm for both systems, and the optimal ratio of polymer to EV-BT was 1:1 by weight (see the SI for data) with the following device structure: ITO/ PEDOT:PSS/ polymer:EV-BT/ LiF/ Al. After independent optimization, POPT:EV-BT devices reach an average efficiency of 1.4% (highest 1.5%) after 40 min of annealing at 80 °C, which is superior to that of GRIM P3HT:EV-BT devices with an average efficiency of 1.1% (highest 1.2%). Rieke P3HT devices fabricated for control purposes only afforded a lower average PCE of 0.70%. It should be noted that Rieke P3HT bilayer devices cannot be fabricated due to the higher solubility of Rieke P3HT in THF compared to GRIM P3HT and POPT. Figure 4 shows representative *J-V* characteristics of BHJ devices made from the three polymers, with device parameters that change minimally up to 100 min of annealing at 80 °C. The POPT device shows a clearly improved J_{sc} over both of the P3HT devices, but its V_{oc} is lower than that of the GRIM P3HT device. The GRIM P3HT device also has a higher efficiency than the Rieke P3HT device due to a larger J_{sc}. Interestingly, the GRIM P3HT device has a lower V_{oc} than the Rieke P3HT device even though the two polymers have similar energy levels.

The larger photocurrent in POPT devices is confirmed by external quantum efficiency (EQE) measurements. As shown in the EQE spectra of Figure 5, the POPT:EV-BT device has greater EQE values (peak EQE = 32%) over the range 400−700 nm compared to both P3HT devices. This range covers the absorption of both POPT and EV-BT, indicating an improved charge generation from both components. Additionally, the broadened absorption of POPT with an earlier onset at 700 nm (see Figure 2) is reflected in the EQE spectrum. The comparison between

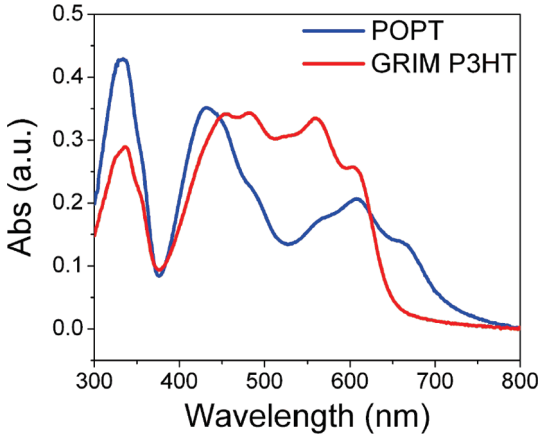

Figure 6. Absorption spectra of POPT (100 nm) and GRIM P3HT (80 nm) blend films with EV-BT at a 1:1 ratio at the optimized BHJ device active layer thickness for each system.

the GRIM P3HT and Rieke P3HT EQE spectra also verifies the improved J_{sc} observed in GRIM P3HT devices, which show higher EQE values (peak EQE = 20%) over the entire range of the active layer absorption from 300 to 650 nm. Integration of the EQE spectrum with respect to the AM 1.5 solar spectrum confirms the J_{sc} as measured under white light illumination. The integrated EQE spectrum of the POPT:EV-BT device gives a J_{sc} of 5.7 mA cm^{-2}, which closely matches the measured J_{sc} of 5.5 mA cm^{-2} in the actual device. Similarly, integration of the EQE spectra of GRIM P3HT and Rieke P3HT devices give 3.1 and 2.2 mA cm^{-2} respectively, in agreement with measured values of 3.0 and 1.9 mA cm^{-2}.

The absorption of the active layer is generally one of the major factors affecting the current generated in the device. As indicated in Table 1, the absorption coefficient of POPT is significantly lower than that of GRIM P3HT. In addition, as seen in Figure 6, the POPT:EV-BT active layer at the optimized device thickness clearly shows reduced absorption compared to the GRIM P3HT:EV-BT blend film. Absorption measurements of the pristine polymers and of the blend films both suggest that optical density most likely cannot account for the improved J_{sc} in POPT devices over GRIM P3HT devices.

Besides differences in absorption, another possible explanation for the higher photocurrent in the POPT device is improved blend morphology that allows for increased donor/acceptor (D/A) interfacial areas for exciton dissociation. Figure 7 shows the AFM height and phase images of films of POPT and GRIM P3HT each blended with EV-BT at a 1:1 ratio. The samples were processed under identical conditions as the optimized BHJ devices. Notably, both samples lack any large scale phase separation, which indicates favorable mixing between the donor polymer and EV-BT. In addition, the blend films show similar domain sizes of 10−20 nm in the phase image. Since there appears to be little difference in total D/A interfacial areas in both samples, morphology most likely does not account for the large difference in photocurrent in devices made from the two polymers.

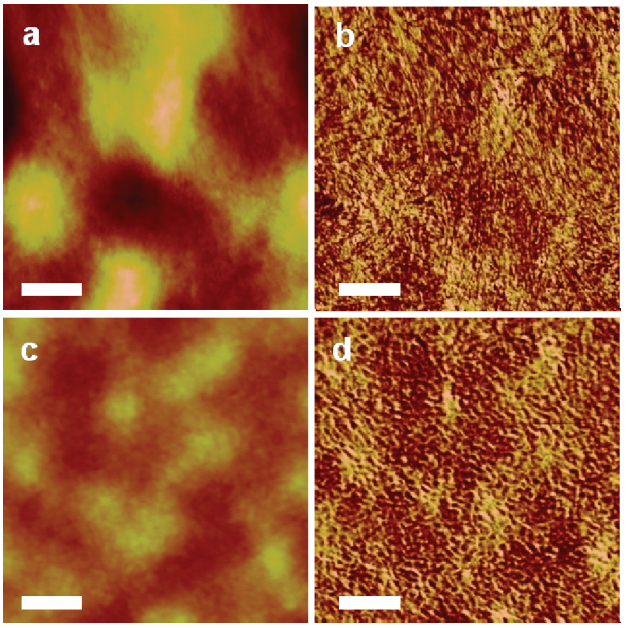

Figure 7. AFM height (left) and phase images (right) of POPT (a, b) and GRIM P3HT (c, d) blends with EV-BT at 1:1 ratios annealed at 80 °C for 100 min. The scale bar is 200 nm.

As the higher photocurrent observed in POPT:EV-BT devices is not expected based on absorption and morphology studies, we performed reverse bias analysis to study the electric-field dependence of the charge generation process in these devices. By applying a larger electric field across the device than the field at J_{sc}, there is an increased driving force for charge separation and collection within the device.[38,39] At sufficiently large reverse bias, the device reaches saturation where all the excitons that reach the D/A interfaces are separated into free charges, and all separated charges are collected at their respective electrode with minimal recombination losses, thus revealing the maximum potential of each polymer:EV-BT device.[38,39]

In reverse bias analysis, the photocurrent is often plotted as a function of effective applied voltage. The photocurrent is defined as $J_{photo} = J_{light} - J_{dark}$, where J_{light} and J_{dark} are current densities of the device measured under illumination and in the dark. The effective applied voltage is defined as $V_{eff} = V_o - V_{app}$, where V_o is the compensation voltage defined as the voltage where $J_{photo} = 0$ and V_{app} is the applied bias. A reverse voltage sweep was applied to the polymer:EV-BT devices, and the photocurrent as a function of effective applied voltage is plotted in Figure 8. Both polymer:EV-BT pairs display higher J_{photo} at higher applied bias as is expected. For the POPT:EV-BT device, J_{photo} saturates relatively quickly at around $V_{eff} = 2$ V. On the other hand, in the GRIM P3HT device, J_{photo} continues to increase and does not reach saturation even at $V_{eff} = 10$ V. More importantly, the J_{photo} of the GRIM P3HT device surpasses that of POPT at $V_{eff} = 9.5$ V, indicating that GRIM P3HT:EV-BT

(38) Blom, P. W. M.; Mihailetchi, V. D.; Koster, L. J. A.; Markov, D. E. *Adv. Mater.* **2007**, *19*, 1551–1566.
(39) Goodman, A. M.; Rose, A. *J. Appl. Phys.* **1971**, *42*, 2823–2830.

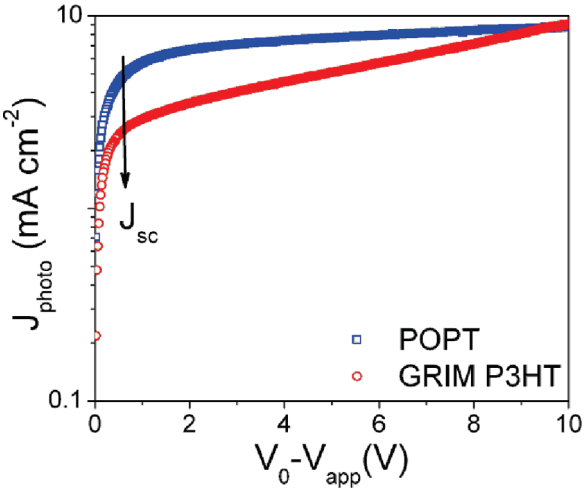

Figure 8. Photocurrent (J_{photo}) versus effective applied voltage (V_0-V_{app}) for optimized BHJ devices of POPT and GRIM P3HT with EV-BT.

can generate more photocurrent than POPT devices. The fact that a GRIM P3HT:EV-BT device can generate higher J_{photo} agrees with expectations based on absorption considerations (see Figure 6 and Table 1) and the observation that the extent of D/A phase separation are similar in the two systems (Figure 7). However, at typical operating voltages, near the J_{sc} position indicated in Figure 8, POPT outperforms GRIM P3HT in terms of charge separation as evidenced by the much higher J_{sc} in POPT:EV-BT devices. Comparing the J_{photo} at low and high fields for these two polymers, it is evident that the dissociation efficiency is much higher for the POPT device, and this device is achieving more of its potential under standard operating conditions.

Discussion

In both bilayer and BHJ devices with EV-BT as acceptor, POPT exhibits superior performance over P3HT with a doubling of the J_{sc} despite its reduced ability to absorb light. Surface morphology probed by AFM suggests that the amount of D/A interfacial area are comparable in the two systems and thus cannot account for the substantial differences in J_{sc}. Reverse bias analysis confirms that GRIM P3HT devices surpass POPT devices in photocurrent generation at high applied field, but charge separation is severely limited at short-circuit condition. Steadily increasing J_{photo} at higher applied bias for the GRIM P3HT system represents a highly field dependent charge separation process in these devices. A strong field dependence in photocurrent can be caused by either the high recombination rate of bound geminate pairs or the buildup of space charge in the device due to unbalanced charge transport.[15,40] In other words, the efficiencies of the GRIM P3HT devices are probably limited by geminate pair recombination and/or space-charge buildup, whereas one or both of these losses are minimized in the POPT device. The electron mobility of EV-BT is lower than the hole mobilities of both POPT and P3HT,[41] and this may be a limiting factor in the performance of these devices. However, the low electron mobility in the acceptor has the same effect on POPT devices and P3HT devices, and thus space-charge buildup most likely is not responsible for the large differences in the performance of the two systems investigated.

A major difference between POPT and P3HT is the pendant phenyl ring on the thiophene moieties of POPT compared to the alkyl chain in P3HT. X-ray diffraction data shows that POPT has an extra $\pi-\pi$ stacking (010) peak at 5.1 Å in addition to the usual (010) peak at 3.8 Å observed in P3HT (see the SI). Both of the (010) peaks in POPT are also broader, indicating a wide range of configurations of the phenyl ring. Out-of-plane twisting of the phenyl ring from the thiophene backbone not only affects the packing of the polymer[22] but also may affect the separation distance between the polymer backbone and an adjacent acceptor molecule. A possible explanation for the higher charge separation efficiency observed in POPT devices is the twisted phenyl ring in POPT that sterically increases the separation distance between the polymer and EV-BT. The larger D/A separation distance forces a larger radius for the geminate pair, which sits partially on the donor and acceptor, respectively. By this mechanism, increasing the radius of the geminate pair may then lower its binding energy and facilitate its dissociation into free charges.

An interesting observation is that the V_{oc} of the EV-BT devices does not fit the trend established in previous studies of polymer/fullerene solar cells. The lower HOMO level of POPT would be expected to afford a higher V_{oc} according to the well-known empirical equation

$$V_{oc} = \frac{1}{e}|E_{HOMO}^{donor} - E_{LUMO}^{acceptor}| - 0.3\ \text{eV}$$

in which the 0.3 eV loss is believed to originate from nonidealities and field-dependent photocurrent in the device.[42−44] Contrary to predictions arising from the use of this empirical V_{oc} equation, both bilayer and bulk-heterojunction POPT devices have a lower V_{oc} than GRIM P3HT devices, suggesting that there may be other factors affecting the V_{oc} of these devices. Therefore, the V_{oc} difference may be due to a variation in charge transfer state energy[45] or the density of free charges, which can affect the internal field of the device or the energy of the free holes and electrons.[46] Another possible explanation

(40) Mihailetchi, V. D.; Xie, H. X.; de Boer, B.; Koster, L. J. A.; Blom, P. W. M. *Adv. Funct. Mater.* **2006**, *16*, 699–708.
(41) Schubert, M.; Steyrleuthner, R.; Bange, S.; Sellinger, A.; Neher, D. *Phys. Status Solidi A* **2009**, *206*, 2743–2749.
(42) Brabec, C. J.; Cravino, A.; Meissner, D.; Sariciftci, N. S.; Fromherz, T.; Rispens, M. T.; Sanchez, L.; Hummelen, J. C. *Adv. Funct. Mater.* **2001**, *11*, 374–380.
(43) Scharber, M. C.; Mühlbacher, D.; Koppe, M.; Denk, P.; Waldauf, C.; Heeger, A. J.; Brabec, C. J. *Adv. Mater.* **2006**, *18*, 789–794.
(44) Dennler, G.; Scharber, M. C.; Ameri, T.; Denk, P.; Forberich, K.; Waldauf, C.; Brabec, C. J. *Adv. Mater.* **2008**, *20*, 579–583.
(45) Vandewal, K.; Gadisa, A.; Oosterbaan, W. D.; Bertho, S.; Banishoeib, F.; Van Severen, I.; Lutsen, L.; Cleij, T. J.; Vanderzande, D.; Manca, J. V. *Adv. Funct. Mater.* **2008**, *18*, 2064–2070.
(46) Koster, L. J. A.; Mihailetchi, V. D.; Ramaker, R.; Blom, P. W. M. *Appl. Phys. Lett.* **2005**, *86*, 123509.

for the lower V_{oc} of the POPT device is a larger shunt resistance in the device, which is reflected by the larger slope of the *J-V* curve near 0 V. The larger shunt resistance may also be responsible for the lower FF in the POPT device. In addition, it is observed that the V_{oc} of GRIM P3HT and Rieke P3HT devices are different even as the two polymers share the same energy levels and optical band gaps. This discrepancy further suggests that the V_{oc} in OPV devices is dependent on factors other than the energy levels of the donor and the acceptor and that the commonly used empirical equation based on donor and acceptor energy levels is not sufficient to predict the device V_{oc}.

Regardless of which polymer is blended with EV-BT, there is no large scale phase separation observed in AFM images. Using a low annealing temperature of 80 °C, POPT:EV-BT device efficiencies can be improved from an initially low efficiency of 0.7% before annealing to 1.4% after annealing for 40−100 min. The same trend of increasing efficiency with annealing is observed in devices made from GRIM P3HT (see the SI). The favorable mixing between the polymers and EV-BT allows for some control of the blend morphology through processing techniques such as thermal annealing, and this nanoscale level miscibility with the polymer is a major advantage of the small molecule vinazene derivatives versus polymeric acceptors.

Conclusions

In both bilayer and BHJ devices using EV-BT as the acceptor, POPT outperforms GRIM P3HT with a higher J_{sc} and higher overall efficiency despite reduced active layer absorption. Blend morphologies observed under AFM indicate similar length scales of phase separation for the two systems. Reverse bias photocurrent analysis confirms that GRIM P3HT devices have the potential to achieve higher photocurrents, but this potential is not attained under standard operating conditions. Since POPT and GRIM P3HT have similar charge mobilities, the strong field dependence of the photocurrent in GRIM P3HT devices is most likely not caused by space-charge buildup but instead due to geminate pair recombination, which is limiting the P3HT device efficiency. In contrast, the POPT:EV-BT device has a weaker field dependence and thus manages to realize more of its potential, achieving a higher dissociation efficiency at short circuit condition and an overall better performance. One distinct difference between P3HT and POPT is that the phenyl ring on POPT can twist out of plane perpendicular to the polymer backbone, thus affecting the way that geminate pairs are separated at the D/A interface. This hypothesis is currently being investigated for this D/A combination as well as others. The comparison between POPT and P3HT highlights the need for further understanding of D/A pair interactions and the effect it has on charge separation processes in polymer solar cells. Considerations based on absorption, mobility, energy levels, and morphology are not sufficient to accurately predict the device performance of any material combination.

Acknowledgment. This work was supported by the U.S. Department of Energy under Contract No. DE-AC02-05CH11231 and by the Center for Advanced Molecular Photovoltaics (Award No KUS-C1-015-21), supported by King Abdullah University of Science and Technology (KAUST). C.H.W. and T.W.H. thank the National Science Foundation for Fellowship support.

Supporting Information Available: Synthetic details, additional absorption spectra, AFM figures, device data, and comparison with Rieke P3HT. This material is available free of charge via the Internet at http://pubs.acs.org.